

Syntheses, Structure, Some Band Gaps, and Electronic Structures of CsLnZnTe₃ (Ln = La, Pr, Nd, Sm, Gd, Tb, Dy, Ho, Er, Tm, Y)

Jiyong Yao,[†] Bin Deng,[†] Leif J. Sherry,[†] Adam D. McFarland,[†] Donald E. Ellis,^{†,‡} Richard P. Van Duyne,[†] and James A. Ibers^{*†}

Department of Chemistry and Department of Physics & Astronomy, Northwestern University, 2145 Sheridan Road, Evanston, Illinois 60208-3113

Received May 14, 2004

Eleven new quaternary rare-earth tellurides, CsLnZnTe₃ (Ln = La, Pr, Nd, Sm, Gd, Tb, Dy, Ho, Er, Tm, and Y), were prepared from solid-state reactions at 1123 K. These isostructural materials crystallize in the layered KZrCuS₃ structure type in the orthorhombic space group *Cmcm*. The structure is composed of LnTe₆ octahedra and ZnTe₄ tetrahedra that share edges to form ∞ [LnZnTe₃] layers. These layers stack perpendicular to [010] and are separated by layers of face- and edge-sharing CsTe₈ bicapped trigonal prisms. There are no Te–Te bonds in the structure of these CsLnZnTe₃ compounds so the formal oxidation states of Cs/Ln/Zn/Te are 1+/3+/2+/2–. Optical band gaps of 2.13 eV for CsGdZnTe₃ and 2.12 eV for CsTbZnTe₃ were deduced from single-crystal optical absorption measurements. A first-principles calculation of the density of states and the frequency-dependent optical properties was performed on CsGdZnTe₃. The calculated band gap of 2.1 eV is in good agreement with the experimental value. A quadratic fit for the lanthanide contraction of the Ln–Te distance is superior to a linear one if the closed-shell atom is included.

Introduction

Ternary and quaternary rare-earth chalcogenides containing a combination of d- and f-elements have been reviewed recently.¹ These compounds are of interest in solid-state chemistry and materials science because of their physical properties and their rich structural chemistry.

Recently, we reported the syntheses, structure, selected physical properties, and theoretical calculations of a series of CsLnMSe₃ compounds (Ln = rare earth or Y; M = Mn, Zn, Cd, Hg).^{2–5} These compounds, which possess the KZrCuS₃ structure type,⁶ are a new class of transparent magnetic semiconductors that exhibit interesting variations

of their optical properties as a function of M and Ln and also display some unusual magnetic properties. Also, one of these studies reported the first extension to the analogous tellurides, namely to RbYbZnTe₃ and CsYbZnTe₃.⁵ In keeping with predictions from theory,⁴ these Te compounds are darker in color and hence possess narrower band gaps than their Se analogues. However, no measurements of optical properties were made. Here we extend these preliminary studies of the tellurides and report the syntheses, structure, selected band gaps, and electronic structures of CsLnZnTe₃.

Experimental Section

Syntheses. The following reagents were used as obtained: La (Cerac, 99.9%), Pr (Strem, 99%), Nd (Cerac, 99.9%), Sm (Alfa Aesar, 99.9%), Gd (Alfa Aesar, 99.9%), Tb (Alfa Aesar, 99.9%), Dy (Alfa Aesar, 99.9%), Ho (Alfa Aesar, 99.9%), Er (Strem, 99.9%), Tm (Strem, 99.9%), Y (Alfa Aesar, 99.9%), Zn (Johnson Matthey, 99.99%), Te (Aldrich, 99.5%), and CsCl (Aldrich, 99.99%). The starting materials were 0.5 mmol of Zn, 1.0 mmol of Ln, 2.0 mmol of Te, and 200 mg of CsCl. The reactants were loaded into fused-silica tubes under an Ar atmosphere in a glovebox.

(6) Mansuetto, M. F.; Keane, P. M.; Ibers, J. A. *J. Solid State Chem.* **1992**, *101*, 257–264.

* To whom correspondence should be addressed. E-mail: ibers@chem.northwestern.edu.

[†] Department of Chemistry.

[‡] Department of Physics & Astronomy.

(1) Mitchell, K.; Ibers, J. A. *Chem. Rev.* **2002**, *102*, 1929–1952.

(2) Huang, F. Q.; Mitchell, K.; Ibers, J. A. *Inorg. Chem.* **2001**, *40*, 5123–5126.

(3) Mitchell, K.; Haynes, C. L.; McFarland, A. D.; Van Duyne, R. P.; Ibers, J. A. *Inorg. Chem.* **2002**, *41*, 1199–1204.

(4) Mitchell, K.; Huang, F. Q.; McFarland, A. D.; Haynes, C. L.; Somers, R. C.; Van Duyne, R. P.; Ibers, J. A. *Inorg. Chem.* **2003**, *42*, 4109–4116.

(5) Mitchell, K.; Huang, F. Q.; Caspi, E. N.; McFarland, A. D.; Haynes, C. L.; Somers, R. C.; Jorgensen, J. D.; Van Duyne, R. P.; Ibers, J. A. *Inorg. Chem.* **2004**, *43*, 1082–1089.

Table 1. Crystal Data and Structure Refinements for CsLnZnTe₃^a

	CsLaZnTe ₃	CsPrZnTe ₃	CsNdZnTe ₃	CsSmZnTe ₃	CsGdZnTe ₃	CsTbZnTe ₃	CsDyZnTe ₃	CsHoZnTe ₃	CsErZnTe ₃	CsTmZnTe ₃	CsYZnTe ₃
fw	719.99	721.99	725.32	731.43	738.33	740.00	743.58	746.01	748.34	750.01	669.99
<i>a</i> (Å)	4.5364(4)	4.4896(5)	4.4702(5)	4.4368(5)	4.4161(4)	4.3992(4)	4.3838(4)	4.3761(14)	4.3604(8)	4.3471(7)	4.3864(3)
<i>b</i> (Å)	16.6203(15)	16.647(2)	16.6648(17)	16.6840(17)	16.7148(15)	16.7044(14)	16.7090(14)	16.721(5)	16.706(3)	16.712(3)	16.7115(12)
<i>c</i> (Å)	12.0854(11)	11.9294(15)	11.8656(12)	11.7724(12)	11.6989(11)	11.6634(9)	11.6194(10)	11.582(4)	11.534(2)	11.5157(19)	11.6102(8)
<i>V</i> (Å ³)	911.19(14)	891.61(18)	883.93(16)	871.44(16)	863.55(14)	857.10(12)	851.11(13)	847.5(5)	840.2(3)	836.6(2)	851.07(10)
ρ_c (g/cm ³)	5.248	5.379	5.450	5.575	5.679	5.735	5.803	5.847	5.916	5.955	5.229
μ (cm ⁻¹)	205.09	216.33	221.83	232.81	243.74	250.71	257.17	263.46	271.46	278.36	237.91
<i>z</i>	0.03	0.05	0.05	0.04	0.03	0.03	0.03	0.03	0.05	0.05	0.02
<i>R</i> (<i>F</i>) ^b	0.0242	0.0354	0.0287	0.0282	0.0192	0.0229	0.0237	0.0268	0.0319	0.0309	0.0169
<i>R</i> _w (<i>F</i> _o) ^c	0.0590	0.0873	0.0737	0.0696	0.0553	0.0567	0.0583	0.0582	0.0822	0.0779	0.0388

^a For all structures, *Z* = 4, space group = *Cmcm*, *T* = 153(2) K, and λ = 0.71073 Å. ^b $R(F) = \sum ||F_o| - |F_c|| / \sum |F_o|$ for $F_o^2 > 2\sigma(F_o^2)$. ^c $R_w(F_o^2) = \{ \sum [w(F_o^2 - F_c^2)] / \sum w F_o^4 \}^{1/2}$ for all data. $w^{-1} = \sigma^2(F_o^2) + (zP)^2$, where $P = (\max(F_o^2, 0) + 2 \times F_c^2) / 3$.

These tubes were sealed under a 10⁻⁴ Torr atmosphere and then placed in a computer-controlled furnace. The samples were heated to 1123 K in 30 h, kept at 1123 K for 96 h, slowly cooled at 4 K/h to 573 K, and then cooled to room temperature. The CsLnZnTe₃ compounds crystallized as dark-red needles or plates. Yields varied from 20% to 40% based on Ln. Analyses of these compounds with an EDX-equipped Hitachi S-3500 SEM showed the presence of Cs, Ln, Zn, and Te, but no Cl. All these compounds are air sensitive, decomposing after a few hours of exposure.

Crystallography. Single-crystal X-ray diffraction data were obtained with the use of graphite-monochromatized Mo K α radiation (λ = 0.71073 Å) at 153 K on a Bruker Smart-1000 CCD diffractometer⁷ in the manner described for the Se analogues. The exposure times varied from 10 to 20 s/frame. Face-indexed absorption corrections were carried out numerically with the program XPREP.⁸ The structures were solved with the direct methods program SHELXS and refined with the full-matrix least-squares program SHELXL of the SHELXTL suite of programs.⁸ Additional crystallographic details are given in Table 1, and Table 2 presents selected bond distances for CsLnZnTe₃ (Ln = La, Pr, Nd, Sm, Gd, Tb, Dy, Ho, Er, Tm, Y).

Optical Microspectroscopy Measurements. Selected single crystals of CsTbZnTe₃ and CsGdZnTe₃ were face-indexed, and their dimensions were measured by means of the video attachment of a Bruker Smart-1000 CCD diffractometer. Crystal dimensions were ([100], [010], [001]): CsGdZnTe₃ 260, 14, 90 μ m; CsTbZnTe₃ 330, 32, 46 μ m. In the manner described previously,^{3,4} absorption measurements on these single crystals with polarized light were performed, and optical band gaps were calculated by the linear regression method. The absorbance spectra of both the (010) and (001) crystal planes for CsTbZnTe₃ (light perpendicular to the *ac* and *ab* crystal planes, respectively) and the spectrum of the (010) crystal plane of CsGdZnTe₃ were recorded. From electronic structure calculations (see below), these compounds are direct band-gap semiconductors so the optical data were manipulated accordingly.

Theoretical Calculations. Calculations for CsGdZnTe₃ were performed by means of the FP-LAPW method,^{9,10} as implemented in the WIEN2k code.¹¹ Included were local orbitals for high-lying semicore states. The exchange-correlations were treated in the local density approximation (LDA) within density-functional theory by

parametrization.¹² There were minimal differences if the exchange-correlations were obtained from the generalized gradient approximation (GGA).¹³ The muffin-tin radii were 3.0, 2.8, 2.3, and 2.69 bohr for Cs, Gd, Zn, and Te, respectively. The plane-wave expansion cutoffs for wave functions (*K*max) and for the densities and potentials (*G*max) were chosen as 7 and 14, respectively. In order to overcome the shortcomings of the LDA, which always puts the 4f states around the Fermi energy and yields a fractional occupation, an open-core treatment was used in which the potential was shifted by a constant. The resulting eigenvalues were also shifted by this constant. The electron density was not affected at all. Although this open-core treatment eliminates the problem that 4f states show around the Fermi energy level, it makes impossible the study of the optical transitions related to the 4f states. Brillouin-zone integrations with self-consistency cycles were performed by means of a tetrahedron method¹⁴ with the use of 200 *k* points throughout the Brillouin zone. For the calculation of the optical properties, 800 *k* points throughout the Brillouin zone were used. The frequency-dependent optical properties were obtained with the use of the joint density of states (JDOS) weighted by the dipole matrix elements of the optical transitions.¹⁵ In this calculation the allowed and forbidden optical transitions were taken into account.

Results and Discussion

Syntheses. The quaternary metal tellurides CsLnZnTe₃ (Ln = La, Pr, Nd, Sm, Gd, Tb, Dy, Ho, Er, Tm, and Y) were prepared at 1123 K by the reactive flux method¹⁶ with a CsCl flux added to aid crystallization. Efforts to synthesize CsCeZnTe₃ were unsuccessful. The synthesis of CsYbZnTe₃ was reported previously.⁵ In the CsLnMSe₃ compounds it was found that as the atomic radius of the transition metal increased so did the radius of the rare earth in order to maintain the anionic framework of edge-sharing MSe₄ tetrahedra and LnSe₆ octahedra and hence the stability of the structure. Thus, the CsLnZnSe₃ compounds could not be synthesized for the Ln elements lighter and hence larger

- (7) SMART Version 5.054 Data Collection and SAINT-Plus Version 6.45a Data Processing Software for the SMART System; Bruker Analytical X-ray Instruments, Inc.: Madison, WI, 2003.
 (8) Sheldrick, G. M. SHELXTL DOS/Windows/NT Version 6.14; Bruker Analytical X-ray Instruments, Inc.: Madison, WI, 2003.
 (9) Wimmer, E.; Krakauer, H.; Weinert, M.; Freeman, A. J. *Phys. Rev. B* **1981**, *24*, 864–875.
 (10) Weinert, M.; Wimmer, E.; Freeman, A. J. *Phys. Rev. B* **1982**, *26*, 4571–4578.

- (11) Blaha, P.; Schwarz, K.; Madsen, G. K.; Kvasnicka, D.; Luitz, J. WIEN2k. An Augmented Plane Wave + Local Orbitals Program for Calculating Crystal Properties; Karlheinz Schwarz, Techn. Universität Wien: Vienna, Austria, 2001.
 (12) Perdew, J. P.; Wang, Y. *Phys. Rev. B: Condens. Matter* **1992**, *45*, 13244–13249.
 (13) Perdew, J. P.; Burke, K.; Ernzerhof, M. *Phys. Rev. Lett.* **1996**, *77*, 3865–3868.
 (14) Blöchl, P. E.; Jepsen, O.; Andersen, O. K. *Phys. Rev. B: Condens. Matter* **1994**, *49*, 16223–16233.
 (15) Ambrosch-Draxl, C.; Majewski, J. A.; Vogl, P.; Leising, G. *Phys. Rev. B: Condens. Matter* **1995**, *51*, 9668–9676.
 (16) Sunshine, S. A.; Kang, D.; Ibers, J. A. *J. Am. Chem. Soc.* **1987**, *109*, 6202–6204.

Table 2. Selected Bond Distances (Å) for CsLnZnTe₃^a

	CsLaZnTe ₃	CsPrZnTe ₃	CsNdZnTe ₃	CsSmZnTe ₃	CsGdZnTe ₃	CsTbZnTe ₃	CsDyZnTe ₃	CsHoZnTe ₃	CsErZnTe ₃	CsTmZnTe ₃	CsYbZnTe ₃	CsYZnTe ₃
Cs–Te1 × 4	3.8476(5)	3.8470(6)	3.8463(5)	3.8461(6)	3.8465(4)	3.8460(5)	3.8462(5)	3.8462(8)	3.8405(7)	3.8425(7)	3.8425(9)	3.8471(3)
Cs–Te1 × 2	4.2665(6)	4.2111(7)	4.1870(6)	4.1539(6)	4.1280(5)	4.1150(5)	4.1012(5)	4.089(1)	4.0739(8)	4.0674(8)	4.066(1)	4.0968(3)
Cs–Te2 × 2	3.8008(7)	3.7947(8)	3.7948(7)	3.7933(8)	3.7986(6)	3.7935(6)	3.7938(6)	3.797(1)	3.795(1)	3.7933(9)	3.790(1)	3.7977(4)
Ln–Te1 × 4	3.2039(3)	3.1616(4)	3.1467(3)	3.1188(4)	3.1025(3)	3.0874(3)	3.0727(3)	3.0653(7)	3.0525(5)	3.0414(5)	3.0328(6)	3.0732(2)
Ln–Te2 × 2	3.1739(3)	3.1394(4)	3.1245(3)	3.1032(3)	3.0859(3)	3.0775(3)	3.0672(3)	3.0583(9)	3.0462(5)	3.0426(5)	3.0417(5)	3.0644(2)
Zn–Te1 × 2	2.6486(7)	2.6481(8)	2.6469(7)	2.6457(8)	2.6436(6)	2.6430(6)	2.6422(6)	2.6392(9)	2.6336(9)	2.6355(8)	2.636(1)	2.6391(4)
Zn–Te2 × 2	2.8063(7)	2.7842(8)	2.7771(7)	2.7631(8)	2.7576(6)	2.7481(7)	2.7402(7)	2.7390(9)	2.732(1)	2.723(1)	2.722(1)	2.7450(4)

^aThe bond distances in CsYbZnTe₃ are taken from the literature.⁵

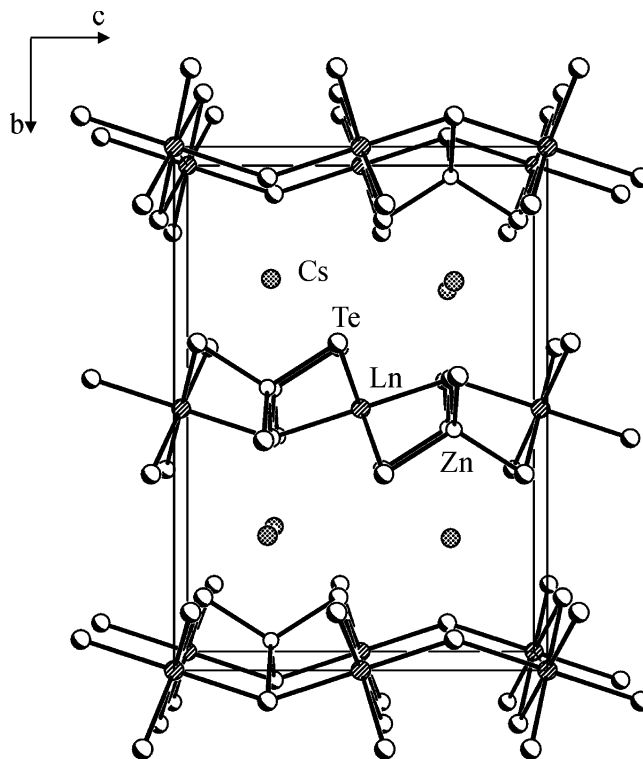
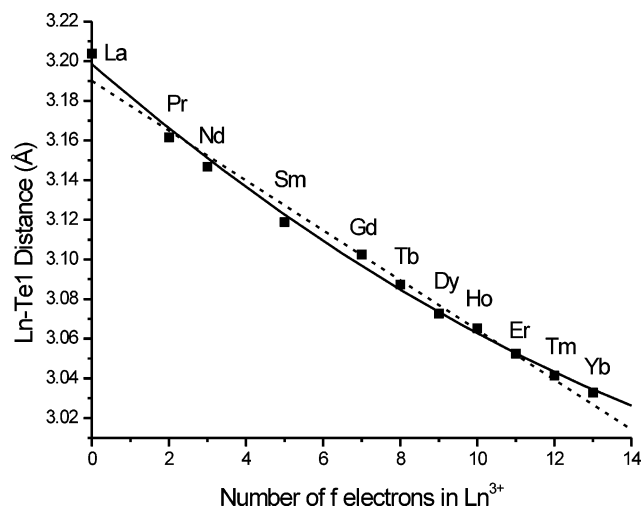
Figure 1. Unit cell of CsLnZnTe₃ viewed down [100].

Figure 2. Ln–Te1 bond distances (Å) in CsLnZnTe₃ vs the number of f electrons in the Ln³⁺ ion. The dashed line is the linear least-squares fit, and the solid line is the quadratic least-squares fit for 0 ≤ n ≤ 13.

than Sm, whereas the CsLnHgSe₃ compounds could not be synthesized for the Ln elements heavier and hence smaller than Ho. Obviously, the larger tetrahedral and octahedral holes in the Te layers are more accommodating compared with the Se layers because the present CsLnZnTe₃ compounds have been synthesized over the entire range of Ln elements.

Structures. The structure of these isostructural CsLnZnTe₃ compounds is illustrated in Figure 1. It is the layered KZrCuS₃ structure type and is composed of LnTe₆ octahedra and ZnTe₄ tetrahedra that share edges to form ²[LnZnTe₃] layers. These layers stack perpendicular to [010] and are separated by layers of face- and edge-sharing CsTe₈ bicapped

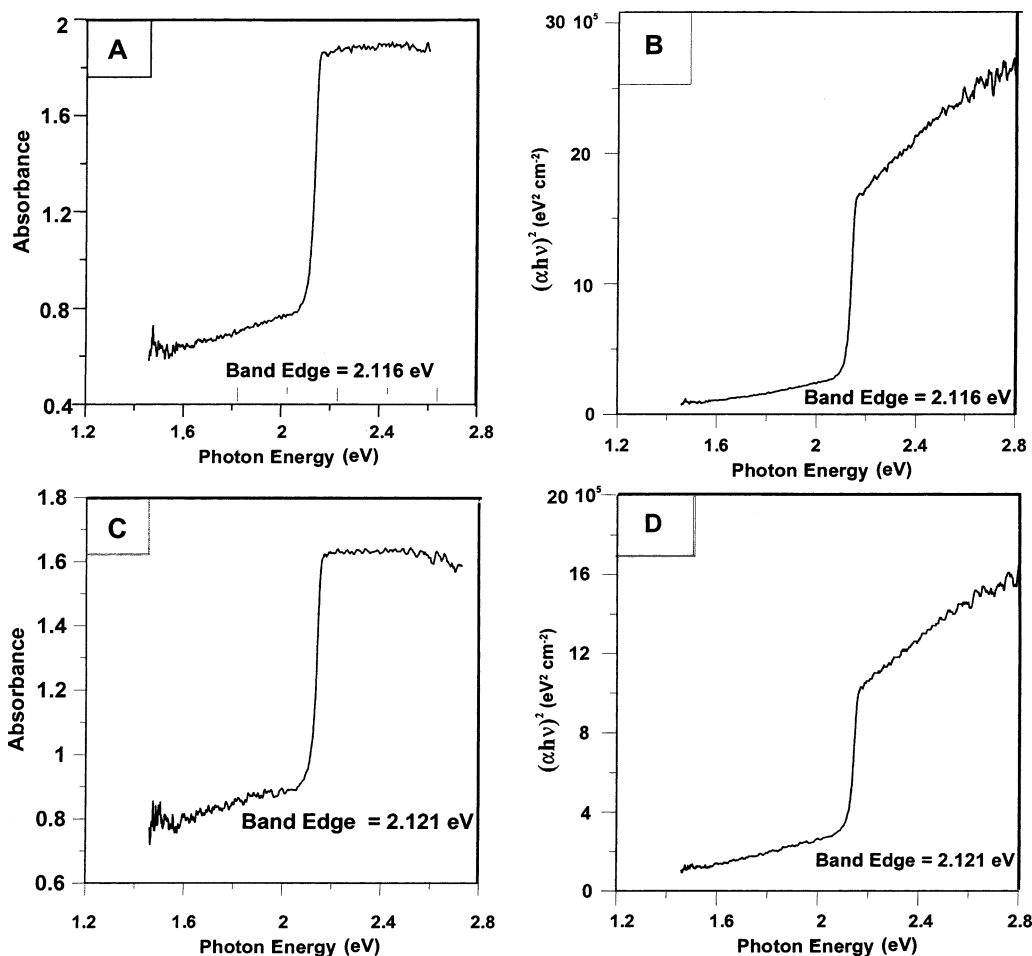


Figure 3. Optical absorption spectra and band-gap calculation for CsTbZnTe₃ crystal. A and C show absorption spectra along the [010] and [001] directions, respectively, and B and D show plots of absorption data for these same directions.

trigonal prisms. The Ln atoms are coordinated to a slightly distorted octahedron of six Te atoms, whereas the Zn atoms are coordinated to a distorted tetrahedron of four Te atoms (Table 2). The structural details have been illustrated earlier.^{2–4} Selected bond distances for these 11 compounds as well as for Ln = Yb⁵ are listed in Table 2. These bond lengths are normal. The ranges of distances are La–Te, 3.1739(3)–3.2039(3) Å; Pr–Te, 3.1394(4)–3.1616(4) Å; Nd–Te, 3.1245(3)–3.1467(3) Å; Sm–Te, 3.1032(3)–3.1188(4) Å; Gd–Te, 3.0859(3)–3.1025(3) Å; Tb–Te, 3.0775(3)–3.0874(3) Å; Dy–Te, 3.0672(3)–3.0727(3) Å; Ho–Te, 3.0583(9)–3.0653(7) Å; Er–Te, 3.0462(5)–3.0525(5) Å; Tm–Te, 3.0414(5)–3.0426(5) Å; Y–Te, 3.0644(2)–3.0732(2) Å; Zn–Te, 2.6336(9)–2.8063(7) Å; and Cs–Te 3.7933(8)–4.2665(6) Å. These ranges are consistent, for example, with those of 3.133(1)–3.2005(7) Å for La–Te in BaLaCuTe₃;¹⁷ 3.377(1)–3.379(2) Å for Pr–Te in PrSeTe₂;¹⁸ 3.1496(4)–3.2732(5) Å for Nd–Te in Nd₂Te₃;¹⁹ 3.0756(5)–3.1388(7) Å for Sm–Te in BaSm₂Te₄;²⁰ 3.0593(4)–3.1247-

(6) Å for Gd–Te in BaGd₂Te₄;²⁰ 3.0424(9)–3.1099(14) Å for Tb–Te in BaTb₂Te₄;²⁰ 3.0343(11)–3.1028(11) Å for Dy–Te in BaDy₂Te₄;²⁰ 3.0230(8)–3.0923(8) Å for Ho–Te in BaHo₂Te₄;²⁰ 3.0115(11)–3.0832(11) Å for Er–Te in BaEr₂Te₄;²⁰ 2.9987(8)–3.0715(9) Å for Tm–Te in BaTm₂Te₄;²⁰ 3.0084(6)–3.0650(5) Å for Y–Te in BaYCuTe₃;¹⁷ 2.6819(5) Å for Zn–Te in KCuZnTe₂;²¹ and 3.693(1)–4.155(2) Å for Cs–Te in Cs₃Tb₇Te₁₂.²² Because there are no Te–Te bonds in the structure, oxidation states of 1+, 3+, 2+, and 2– can be assigned to Cs, Ln, Zn, and Te, respectively.

Lanthanide Contraction. The lanthanide contraction is clearly evident in the lattice constants and the Ln–Te bond distances. For the RbLnSe₂ compounds,²³ a quadratic expression $d(\text{Ln–Se}) = A_0 - A_1n + A_2n^2$, where $0 \leq n \leq 14$ is the number of f electrons, provides a better fit to the lanthanide contraction than does a linear one $d(\text{Ln–Se}) = B_0 - B_1n$, although not if the closed-shell atoms La and Lu are excluded (i.e., $1 \leq n \leq 13$). Such a nonlinear relationship was described previously,^{24,25} where it was ascribed to crystal-

(17) Yang, Y.; Ibers, J. A. *J. Solid State Chem.* **1999**, *147*, 366–371.

(18) Fokwa, B. P. T.; Doert, T.; Simon, P.; Söhnel, T.; Böttcher, P. Z. *Anorg. Allg. Chem.* **2002**, *628*, 2612–2616.

(19) Ijjaali, I.; Ibers, J. A. *Acta Crystallogr. Sect. C: Cryst. Struct. Commun.* **2002**, *58*, i124–i125.

(20) Narducci, A. A.; Yang, Y.; Digman, M. A.; Sipes, A. B.; Ibers, J. A. *J. Alloys Compd.* **2000**, *303–304*, 432–439.

(21) Heulings, H. R., IV; Li, J.; Proserpio, D. M. *Main Group Met. Chem.* **1998**, *21*, 225–229.

(22) Tougaï, O.; Noël, H.; Ibers, J. A. *Solid State Sci.* **2001**, *3*, 513–518.

(23) Deng, B.; Ellis, D. E.; Ibers, J. A. *Inorg. Chem.* **2002**, *41*, 5716–5720.

field contractions of those rare earths lacking spherical symmetry.²⁴ The nonlinear relationship was recently rediscovered.²⁶ A similar analysis was performed on the Ln–Te distances (Table 2) in these CsLnZnTe₃ compounds. Results for the Ln–Te1 distances are shown in Figure 2. The results for the Ln–Te2 distances are similar. Once again, a quadratic fit of $d(\text{Ln}-\text{Te})$ versus n is superior to a linear one if the closed-shell atom, in this case La, is included.

Optical Properties and Electronic Structures. The optical absorption spectra of the (010) and (001) crystal planes for CsTbZnTe₃ are shown in Figure 3. The optical band gap is about 2.12 eV, consistent with the color of the crystal. There is no significant difference between the band gaps along the two different orientations for this compound. For CsGdZnTe₃, the band gap of the (010) crystal plane is 2.13 eV.

The total and partial densities of states (DOS) of CsGdZnTe₃ are shown in Figure 4a. The contributions from the Gd (4f) orbitals are not shown in the total DOS. The Zn (3d) orbitals are highly localized, as can be seen from the sharp peak near -7 eV. The Gd, Zn, and Te orbitals are hybridized in the valence and conduction bands, which can be seen from the overlap among them around the Fermi level. The valence band primarily consists of Te1 (5p) and Te2 (5p) orbitals, whereas the conduction band has most contributions from Gd (5d and 6s) orbitals, Zn (4s and 4p) orbitals, and less significantly from Te (5s and 5p) orbitals. Because Cs has almost no contributions in the DOS, the electronic properties are mainly determined by the two-dimensional $\infty[\text{GdZnTe}_3]$ anionic framework. The band structure of CsGdZnTe₃ (not shown) indicates that the valence-band maximum and conduction-band minimum are both located at the same k point. Thus, the CsLnZnTe₃ compounds are direct band-gap semiconductors, and for each, the lowest optical transition is simply from the valence-band maximum to the conduction-band minimum.

To calculate optical absorption, we considered the interband transitions, with the initial states being the occupied valence-band states and the final states being the unoccupied conduction-band states. Interband transitions are the most important part of optical transitions in direct band-gap semiconductors. The joint density of states (JDOS) is related to a convolution over the valence-band and conduction-band density of states functions. It corresponds to the optical transitions between the valence-band and conduction-band states. The JDOS is zero if the transitions are forbidden or if no initial or final states are present at the transition energy. It is large for allowed transitions between bands with a large DOS at the transition energy. The JDOS of CsGdZnTe₃ is shown in Figure 4b. An optical transition at 2.1 eV can be deduced from this figure. Although the muffin-tin radii were optimized to avoid electron leakage from the Zn and Te

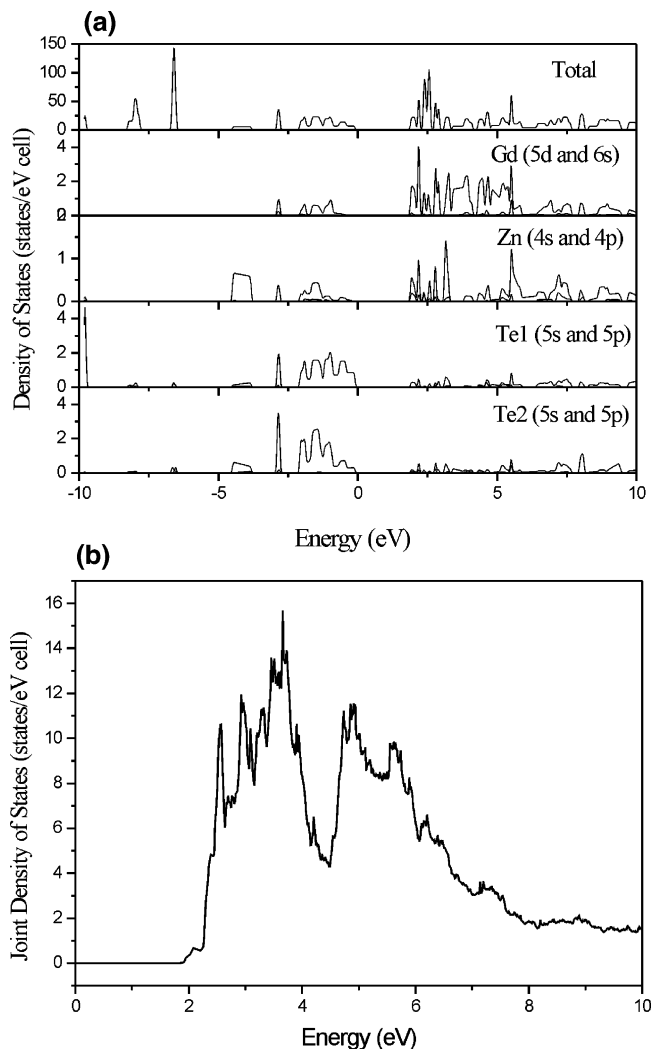


Figure 4. (a) Density of states (DOS) (Fermi level is at zero) and (b) joint density of states (JDOS) of CsGdZnTe₃.

cores, the small peaks in the JDOS around 2.0 eV arise from 0.002 electrons leaking from every Zn core and 0.003 electrons leaking from every Te core. Although the LDA is known to underestimate optical band gaps,^{27,28} the value obtained from the JDOS is in surprisingly close agreement with the experimental value of 2.13 eV.

Previous density functional theory calculations on the CsYMSe₃ ($M = \text{Zn}, \text{Cd}, \text{Hg}$) compounds indicate that the 4p orbitals of Se also contribute mainly to the valence band. Because the sequence of energy levels of p orbitals is $4p(\text{Se}) < 5p(\text{Te})$, the band gaps for the CsLnZnTe₃ compounds should be smaller than those of the CsLnZnSe₃ analogues. This is demonstrated by both the colors and the band gaps obtained for these two series of compounds. The CsLnZnSe₃ compounds are yellow, gray, or red,³ whereas the CsLnZnTe₃ reported here are all dark red. The band gaps measured for selected CsLnZnSe₃ compounds along [010] are around 2.4–2.6 eV,³ whereas the band gaps measured

(24) Gschneidner, K. A., Jr.; Valletta, R. M. *Acta Metall.* **1968**, *16*, 477–484.

(25) Beaudry, B. J.; Gschneidner, K. A., Jr. In *Handbook on the Physics and Chemistry of Rare Earths*; Gschneidner, K. A., Jr., Eyring, LeR., Eds.; Elsevier Science Publishers B.V.: New York, 1978; Vol. 1, pp 173–232.

(26) Quadrelli, E. A. *Inorg. Chem.* **2002**, *41*, 167–169.

(27) Hybertsen, M. S.; Louie, S. G. *Comments Condens. Matter Phys.* **1987**, *13*, 223–247.

(28) Perrin, M.-A.; Wimmer, E. *Phys. Rev. B: Condens. Matter* **1996**, *54*, 2428–2435.

for the present CsLnZnTe₃ compounds are around 2.1 eV. A similar shift of band gaps in the RbLnSe₂ compounds has also been noted.²³

Acknowledgment. This research was supported by National Science Foundation Grant DMR00-96676. Use was made of the Central Facilities supported by the MRSEC program of the National Science Foundation (DMR00-

76097) at the Materials Research Center of Northwestern University.

Supporting Information Available: Crystallographic files in CIF format for CsLnZnTe₃ (Ln = La, Pr, Nd, Sm, Gd, Tb, Dy, Ho, Er, Tm, Y). This material is available free of charge via the Internet at <http://pubs.acs.org>.

IC040071P